
01 Jan 2015

Effect of Nitrogen on Properties of Na₂O-CaO-SrO-ZnO-SiO₂ Glasses

Ahmed Bachar


Cyrille Mercier

Arnaud Tricoteaux

Jean Christophe Hornez

et. al. For a complete list of authors, see https://scholarsmine.mst.edu/che_bioeng_facwork/1130

Follow this and additional works at: https://scholarsmine.mst.edu/che_bioeng_facwork

 Part of the [Biochemical and Biomolecular Engineering Commons](#), and the [Biomedical Devices and Instrumentation Commons](#)

Recommended Citation

A. Bachar et al., "Effect of Nitrogen on Properties of Na₂O-CaO-SrO-ZnO-SiO₂ Glasses," *Journal of the American Ceramic Society*, vol. 98, no. 3, pp. 748 - 757, Wiley, Jan 2015.

The definitive version is available at <https://doi.org/10.1111/jace.13361>

This Article - Journal is brought to you for free and open access by Scholars' Mine. It has been accepted for inclusion in Chemical and Biochemical Engineering Faculty Research & Creative Works by an authorized administrator of Scholars' Mine. This work is protected by U. S. Copyright Law. Unauthorized use including reproduction for redistribution requires the permission of the copyright holder. For more information, please contact scholarsmine@mst.edu.

Effect of Nitrogen on Properties of Na₂O–CaO–SrO–ZnO–SiO₂ Glasses

Ahmed Bachar,^{‡,††} Cyrille Mercier,[‡] Arnaud Tricoteaux,[‡] Jean-Christophe Hornez,[‡] Anne Leriche,[‡] Claudine Follet,[‡] Bertrand Revel,[§] Stuart Hampshire,^{¶,†,***} and Mark R. Towler^{||}

[‡]Laboratoire des Matériaux Céramiques et Procédés Associés (LMCPA), Université de Valenciennes et du Hainaut-Cambrésis, Valenciennes, France

[§]Centre Commun de Mesure RMN, Université Lille1 Sciences et Technologies, Cité Scientifique, Villeneuve d'Ascq, France

[¶]Materials and Surface Science Institute (MSSI), University of Limerick, Limerick, Ireland

^{||}Department of Mechanical and Industrial Engineering, Ryerson University, Toronto, Canada

^{††}Lab. Conditions Extrêmes et Matériaux: Haute Température et Irradiation (CEMHTI), CNRS-Université d'Orléans, Orléans, France

Glasses in the Na₂O–CaO–SrO–ZnO–SiO₂ system have previously been investigated for suitability as a reagent in Al-free glass polyalkenoate cements (GPCs). These materials have many properties that offer potential in orthopedics. However, their applicability has been limited, to date, because of their poor strength. This study was undertaken with the aim of increasing the mechanical properties of a series of these Zn-based GPC glasses by doping with nitrogen to give overall compositions of: 10Na₂O–10CaO–20SrO–20ZnO–(40–3x)SiO₂–xSi₃N₄ (x is the no. of moles of Si₃N₄). The density, glass-transition temperature, hardness, and elastic modulus of each glass were found to increase fairly linearly with nitrogen content. Indentation fracture resistance also increases with nitrogen content according to a power law relationship. These increases are consistent with the incorporation of N into the glass structure in threefold coordination with silicon resulting in extra cross-linking of the glass network. This was confirmed using ²⁹Si MAS-NMR which showed that an increasing number of Q² units and some Q³ units with extra bridging anions are formed as nitrogen content increases at the expense of Q¹ units. A small proportion of Zn ions are found to be in tetrahedral coordination in the base oxide glass and the proportion of these increases with the presence of nitrogen.

I. Introduction

Bioglass^{®1} is known to bond to living bone in the body through formation of an apatite layer on its surface^{1–5} and this has accelerated the search for new bioactive glasses and glass-ceramics with enhanced properties. However, the low strength and inherent brittleness of Bioglass[®] has restricted its use to nonload-bearing applications.^{1,2}

Glass Polyalkenoate Cements (GPCs) have been used for many years in dentistry and are now finding applicability in orthopedics,^{6,7} and as adhesives for cochlear implants.³ GPCs are formed by the acid-base reaction of an ion leachable fluorine-containing calcium aluminosilicate glass (sometimes containing phosphate ions) with an aqueous solution of polyacrylic acid (PAA).⁸ The acid reacts with and

degrades the glass structure, releasing metal cations into the aqueous phase of the setting cement. Once in the aqueous phase, these cations are cross-linked by the carboxylate groups on the PAA chains to form the cement with a micro-structure consisting of reacted and unreacted glass particles embedded in a hydrated polysalt matrix. The setting reaction of the cements depends critically on the glass composition⁸ with Al³⁺ ions playing an important role. The presence of fluoride in the glass composition is clinically beneficial, because this fluoride ion is released and readily exchanged for the hydroxyl ion of the hydroxyapatite in natural tooth and bone minerals.

Conventional aluminosilicate glass based GPCs have been found unsuitable for application in orthopedics because of the presence of aluminum in the glass phase which is a neurotoxin. Therefore, for these applications, the elimination of Al from the glass is essential. Ternary systems based on zinc silicates often have extensive regions of glass formation and, thus, Al-free GPCs have been synthesized based on calcium zinc silicate glasses.⁹ Zinc oxide is bactericidal and incorporation of zinc oxide into bioactive silicate glasses allows a modification of the ion release behavior depending on pH of the environment, with glasses being relatively stable at neutral pH but dissolving faster under acidic conditions.¹⁰ Zinc oxide, in a silicate glass, can act as an intermediate oxide (either as a network former or modifier)^{10–14} in the same way as alumina. Small additions of ZnO in Na₂O–CaO–SiO₂ glasses have been found to improve the mechanical and chemical durability which is thought to be a consequence of the partial tetrahedral network forming contribution of ZnO.¹⁵

Glass Polyalkenoate Cements based on two different Al-free CaO–ZnO–SiO₂ glasses exhibited handling properties and flexural strengths comparable to conventional GPCs.⁹ One of these CaO–ZnO–SiO₂ glasses, when mixed with PAA to form a GPC, was immersed in simulated body fluid and an amorphous calcium phosphate layer was nucleated on its surface⁹ indicating that the GPC is bioactive in nature.

Strontium (Sr) is a known bone forming agent used in the treatment of osteoporosis, and has been substituted for Ca in a Bioglass[®] to improve properties.¹⁶ To further improve the potential of the Al-free Zn-based GPCs, Ca was substituted by Sr in a series of GPC glass phases¹² to form CaO–SrO–ZnO–SiO₂ glasses. ²⁹Si MAS-NMR analysis indicated that the substitution of Ca by Sr in these glasses did not appear to significantly affect their network connectivity. Evaluation of the subsequent reactivity of these glasses with an aqueous solution of PAA showed that increasing the amount of Sr

P. Colombo—contributing editor

Manuscript No. 35125. Received June 10, 2014; approved October 28, 2014.

**Fellow, The American Ceramic Society.

†Author to whom correspondence should be addressed. e-mail: stuart.hampshire@ul.ie

substituted for Ca resulted in a decrease in working/setting times as a result of faster degradation of the glass phase, which may be attributable to the higher basicity of SrO compared with CaO.

A SiO₂–CaO–ZnO–SrO GPC and two commercial Al-containing GPCs, all with similar setting chemistry, were compared.¹⁷ Working and setting times for the Zn–Sr–based GPC were shorter than the commercial Al-based GPCs, as a result of faster dissolution under acidic conditions, and it had a higher setting exotherm (34°C) compared with the commercial GPCs (29°C). The maximum compressive and flexural strengths for the Zn–Sr–based GPC were lower than commercial GPCs which might make them more suitable for spinal applications. However, the search for higher strength bioactive glasses continues.

One solution to the challenge of low-strength glasses is to incorporate nitrogen into the silicate network.^{18–21} When nitrogen replaces oxygen in aluminosilicate glasses, glass-transition temperature, elastic modulus, and hardness increase linearly with nitrogen content.^{18,19} A study of incorporation of N into a potentially bioactive glass composition has shown that nitrogen increases mechanical properties.²² Oxynitride glass-ceramics have also been shown to exhibit potential bioactivity.²³ The main conclusion is that N may be viewed as a network forming anion taking into account that the effects of nitrogen and modifiers on glass properties are independent.²⁴

The aim of this work was to substitute oxygen by nitrogen in a Na₂O–CaO–SrO–ZnO–SiO₂ glass which has previously been investigated for use in GPCs and to study properties as a function of nitrogen content and the effect of composition on structures of the prepared oxynitride glasses.

II. Experimental Procedure

(1) Glass Synthesis

Oxynitride glasses of molar composition 10Na₂O–10CaO–20SrO–20ZnO–(40–3x)SiO₂–xSi₃N₄ (x is the no. of moles of Si₃N₄) were prepared from reagent grade Na₂CO₃ (purity 99.9%; Merck, Darmstadt, Germany), CaCO₃ (purity 99%; Chimie-Plus-Laboratoire, Denice, France), SrCO₃ (purity 99%; Chimie-Plus-Laboratoire), ZnO (purity 99.9%; Merck), SiO₂ (pure quartz; Merck), and Si₃N₄ (minimum purity 98%; UBE Europe GmbH, Düsseldorf, Germany). The weights of each reagent were calculated taking into account their purity and these are shown in Table I.

The glasses were designed so that constant cation ratios could be maintained independent of nitrogen addition. Thus, the N:O ratio is the only compositional variable which changes and the effects of cation ratio variations on glass structure and properties are eliminated. The compositions of the glasses in atomic % of the elements are shown in Table II.

Initial experiments resulted in high weight losses and a solid residue which had evolved from the melt was analyzed as Zn. Therefore, as the reaction of ZnO and Si₃N₄ results in formation of Zn and N₂, base Na₂O–CaO–SrO–SiO₂ glasses were first prepared without zinc oxide followed by addition of silicon nitride to incorporate nitrogen into the glasses and

finally addition of zinc oxide. The different stages of glass synthesis are as follows:

1. Synthesis of base oxide glasses without ZnO with molar proportions: 10Na₂O–10CaO–20SrO–(40–3x)SiO₂. These were melted in air in platinum crucibles at 1450°C for 1 h.
2. Milling and mixing of these base oxide glasses with varying amounts (x = 1, 2, 3, 4) of silicon nitride (Si₃N₄) powder. The powders were weighed and mixed in a glass dish using a magnetic stirrer in 50 mL isopropanol and then the alcohol evaporated by heating. Powder batches were pressed under 300 MPa pressure and small pellets of 1 cm height were obtained.
3. The pellets were melted in boron nitride lined graphite crucibles in a vertical tube furnace under flowing high-purity N₂ at 1400°C for 15 min. The crucible was removed from the furnace and the glass was poured onto a steel plate to form a solid disk.
4. The oxynitride glass disk was crushed and placed in a planetary mill to form a powder which was mixed with the appropriate amount of ZnO using a magnetic stirrer in 50 mL isopropanol and then the alcohol evaporated by heating. Powder batches were pressed under 300 MPa pressure and small pellets of 1 cm height were obtained.
5. The pellets containing all the components were melted in boron nitride lined graphite crucibles in a vertical tube furnace under flowing high-purity N₂ at 1400°C for 15 min. The crucible was removed from the furnace and the glass was poured onto a steel plate to form a solid disk.
6. Following casting, the glasses were then annealed, just below their glass-transition temperature for 1 h, to stabilize the glass by eliminating stresses that would have remained after rapid cooling.

(2) Glass Characterization

(A) *X-ray Diffraction Analysis*: To determine if there were any crystalline phases present, samples were analyzed using X-ray diffraction (PanAlytical X-ray diffractometer, PanAlytical, Almelo, the Netherlands) with monochromated CuK_α (λ = 1.54056 Å) radiation over a range of 2θ of 20°–80° with a speed of 2.4°/min. Data were analyzed using X'pert Quantify software.

(B) *Elemental Analysis by Wavelength Dispersive Spectroscopy (WDS) and EDS*: The nitrogen concentrations retained in the glasses, shown in Table II (Exp), were determined by electron probe microanalysis (Cameca SX100 electron probe microanalyzer, Gennevilliers Cedex, France) using WDS. All samples were embedded into an epoxy resin, and then polished using SiC papers down to 0.25 μm to provide a completely flat surface. Quantification of N was carried out at 15 kV, 200 nA. A PC2 (Ni/C) crystal was used to detect the K_α X-rays. The standard used for N quantification was BN. For each glass, 10 measurements were performed to evaluate the nitrogen homogeneity and to calculate the average nitrogen content in the glasses. The background noise used for the calculation of the N K_α peak height on the glass samples was measured on a glass without N. The accuracy and detection limits of this method had previously been assessed by analyses of standard Ca–Mg–aluminosilicate glasses containing up to 6143 ppm nitrogen.²⁵

The relative contents of Si, Ca, Na, and O were analyzed on similar prepared embedded polished samples using scanning electron microscopy coupled with energy dispersive spectroscopy (SEM–EDS; Noran System Six-type, Thermo Fisher Scientific, Villebon-sur-Yvette, France), the analyzed area being about 1 μm³.

Table I. Weight Percentages of Oxides/Si₃N₄ Used to Prepare Na–Ca–Sr–Zn–Si–O–N_x Glasses

| Wt. % | Na ₂ O | CaO | SrO | ZnO | SiO ₂ | Si ₃ N ₄ |
|-------|-------------------|-------|-------|-------|------------------|--------------------------------|
| BT0 | 11.72 | 11.06 | 32.64 | 18.00 | 26.58 | – |
| BT1 | 11.74 | 11.09 | 32.71 | 18.04 | 25.64 | 0.78 |
| BT2 | 11.77 | 11.12 | 32.79 | 18.07 | 24.69 | 1.56 |
| BT3 | 11.79 | 11.14 | 32.86 | 18.12 | 23.74 | 2.35 |
| BT4 | 11.83 | 11.16 | 32.94 | 18.15 | 22.79 | 3.13 |

Table II. Atomic Percentages of Elements in Na–Ca–Sr–Zn–Si–O–N_x Glasses

| At. % | Na | | Ca | | Sr | | Zn | | Si | | O | | N | |
|-------|------|------------|------|------------|------|------------|------|------------|-------|------------|-------|------------|------|-------------|
| | Th | Exp (±0.2) | Th | Exp (±0.1) | Th | Exp (±0.2) | Th | Exp (±0.2) | Th | Exp (±0.3) | Th | Exp (±0.2) | Th | Exp (±0.04) |
| BT0 | 8.00 | 8.54 | 4.00 | 3.77 | 8.00 | 7.06 | 8.00 | 7.62 | 16.00 | 17.95 | 56.00 | 56.00 | – | – |
| BT1 | 8.03 | 8.83 | 4.01 | 3.99 | 8.03 | 8.48 | 8.03 | 5.03 | 16.06 | 17.06 | 55.02 | 55.99 | 0.8 | 0.62 |
| BT2 | 8.06 | 8.96 | 4.03 | 4.01 | 8.06 | 8.56 | 8.06 | 5.06 | 16.12 | 17.12 | 54.03 | 55.00 | 1.61 | 1.28 |
| BT3 | 8.09 | 8.79 | 4.04 | 4.00 | 8.09 | 8.69 | 8.09 | 5.09 | 16.19 | 17.21 | 53.03 | 54.26 | 2.42 | 1.96 |
| BT4 | 8.13 | 8.85 | 4.06 | 4.03 | 8.13 | 8.73 | 8.13 | 5.13 | 16.26 | 17.34 | 52.03 | 53.29 | 3.25 | 2.63 |

Th, Theoretical; Exp, Experimental

(3) Measurement of Density

The density was measured using a Helium pycnometer. Glasses were crushed before density measurements so that any internal porosity (i.e., bubbles) did not affect the results.

(4) Thermal Analysis

Differential thermal analysis (DTA) was carried out (Setaram Setsys 16/18 simultaneous TG/DTA analyzer, Caluire, France) to determine the glass-transition temperature, T_g . Samples of 50 mg were heated at 10°C/min up to 1200°C in alumina crucibles in a flowing nitrogen atmosphere. Al₂O₃ was used as the reference material. The inflexion point of the endothermic drift on the DTA curve is reported as T_g .

(5) Determination of Mechanical Properties

(A) *Measurement of Microhardness:* The microhardness of the investigated samples was measured using a standard Vickers hardness tester (Load Cell Hardness Tester FLC 50V; Future-Tech Corp., Kawasaki, Japan) with a 136° diamond pyramid indenter. The specimens were cut using a low speed diamond saw, dry ground using 1200 grit SiC paper and polished carefully using 6, 3, and 1 μm diamond pastes to obtain smooth glass samples with flat parallel surfaces before indentation. The influence of loading test on hardness (Indentation Size Effect, ISE) was studied for all glasses. Loads were chosen between 25 and 500 g and the loading time was fixed at 15 s. At least five indentations were measured at each load for each sample. An exception was made at 500 g, where 10 indentation measurements were carried out to calculate a mean true Vickers hardness number Hv_0 and standard deviation. Figure 1 shows the effect of load on Hv . Hv_0 is obtained when the measured values of Hv are constant with load. The measurements were carried out under normal atmospheric conditions.

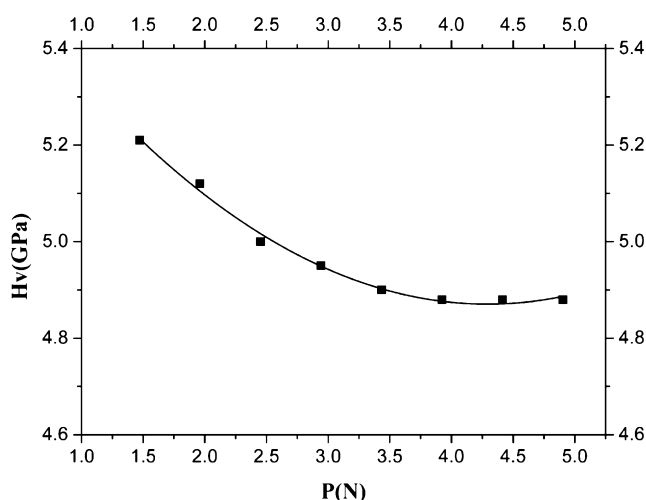


Fig. 1. Variation in Vickers hardness Hv of Na–Ca–Sr–Zn–Si–O–N_x glasses as a function of applied load P .

The Vickers hardness values (in GPa) were calculated from the following equation:

$$Hv = 1.8544 \frac{P}{d^2} \quad (1)$$

where P is the applied load and d is the average length of the two diagonals. The eyepiece on the microscope of the equipment allowed measurements with an estimated accuracy of 0.5 μm for the indentation diagonals.

(B) *Measurement of Young's Modulus:* Young's modulus was measured using a Knoop indentation method which is based on that given by Marshall *et al.*²⁶ The authors describe a method for calculating the hardness, HK, to Young's modulus, E , ratio (HK/ E) of a material from measurements of the Knoop indent diagonals. The decrease in the length of the indent minor diagonal is caused by elastic recovery of the material and, consequently, it can be related to the hardness:modulus ratio by the following equation:

$$\frac{w'}{L'} = \frac{w}{L} - \alpha \frac{HK}{E} \quad (2)$$

where w' and L' are the minor and the major diagonals of the measured Knoop indent, w and L are the minor and major diagonals of the ideal Knoop indent for which $L/w = 7.11$ and α is a constant = 0.45.²⁶

HK is the Knoop hardness calculated by the relationship:

$$HK = 14.229 \frac{P}{L^2} \quad (3)$$

where P is the load.

Bachar *et al.*²⁷ showed that values of Young's modulus measured by Knoop indentation and by ultrasonic methods were very similar but only if the glass is homogeneous and without bubbles. Chicot and Tricoteaux²⁸ also showed that Marshall's method and a depth-sensing indentation method (with both Vickers and spherical indenters) applied to a beta-TCP ceramic gave very similar results. Therefore, measuring Young's modulus by a "local" Knoop indentation method has been found to be more reliable than using a "bulk sample" method (ultrasonic, etc.) where the presence of any bubbles act as defects and skew the results.

(C) Vickers Indentation Fracture (VIF) Resistance:

The Vickers indentation test is often used for determining the fracture toughness of glasses. This method consists in indenting the glass with a Vickers indenter to generate cracks at the extremities of the indent. Afterward, the toughness is calculated from the dimensions of the indent diagonals and of the crack lengths. Because the Vickers Indentation Fracture test is not standard, the calculated value cannot be considered as equivalent to the toughness of the material K_{IC} and therefore it will be referred to as VIF resistance, K_{IF} . Eight Vickers indentations were made at each of 10 loads ranging from 1.472 to 4.905 N on each of the five glasses.

Dimensions of indent diagonals and crack lengths were measured on optical micrographs using the image analysis software ImageJ[®].

The VIF resistance can be calculated from various relationships depending on the load, indent diagonal, crack length, Young's modulus to hardness ratio and on the cracking mode under the indenter. Recently, Bachar *et al.*²⁷ defined a methodology to calculate K_{ifr} for oxynitride and oxyfluoronitride glasses. This methodology allows firstly the cracking mode (Radial-Median, Palmqvist or Intermediate) to be identified and secondly the VIF resistance to be calculated from the appropriate relationship. The authors show that, depending on the cracking mode, K_{ifr} can be calculated from one of the three following relationships: For Radial-median cracks

$$K_{ifr(R-M)} = 0.0154 \left(\frac{E}{HV} \right)^{1/2} \frac{P}{c^{3/2}} \quad (4)$$

For Palmqvist cracks

$$K_{ifr(P)} = 0.0089 \left(\frac{E}{HV} \right)^{2/5} \frac{P}{al^{1/2}} \quad (5)$$

For intermediate cracks

$$K_{ifr(I-M)} = (\alpha - \beta q) f \left(\frac{E}{HV} \right) \frac{P}{a^q c^{(1.5-q)}} \quad (6)$$

where c , a , l are the indent and crack lengths and P is the Vickers indentation load. The identification of the cracking mode and the calculation of the parameters α , β , q , and $f(E/HV)$ is also detailed in the same reference.²⁷

(6) Structural Analysis by ²⁹Si NMR

²⁹Si MAS NMR spectra were recorded at a Larmor frequency of 79.5 MHz using a Bruker (Wissembourg, France) Avance 400 MHz (9.4 T) spectrometer. The spectra were obtained with 96 scans with a pulse length of 1.7 μs (π/6), a relaxation delay of 300 s, and with a spectral width of 25 kHz. For all glasses, the time acquisition of the signal was 15 ms. An exponential linebroadening (LB) factor of 20 Hz was used during spectral processing, the spectral resolution is 6.10 Hz/pt (0.08 ppm). The samples were spun at the magic angle of 54.7° and at spin rates of 5 kHz in 7-mm-outer diameter zirconia rotors, with tetramethylsilane used as reference. Spectral deconvolution was performed with Dmfit software²⁹ which allows an optimization of the reconstructed spectrum. It is possible to change the settings for amplitude, position, full-width at half maximum (FWHM), Gaussian/Lorentzian ratio [xG/(1-x)L] and this allows the software to use these data to simulate the spectrum.

III. Results and Discussion

(1) Glass Synthesis and Appearance of Glasses

Glass synthesis, while involving a number of steps, is successful in producing homogeneous Na-Ca-Sr-Zn-Si oxynitride glasses. Table II compares the elemental analyses of the glasses as designed and after melting. It can be seen that the experimental values of both nitrogen and zinc contents are lower than the theoretical values for each glass composition, which may be attributed to volatilization of Zn and N according to:



Despite the precautions of using different steps for addition of Zn and N, weight losses overall during all steps of

preparation were approximately 0.6% with approximately 25% of the nitrogen lost in each case. The glasses were observed to be transparent but with a gray color which is typical of oxynitride glasses as reported previously¹⁸⁻²¹ and is due to the presence of N. X-ray diffraction analysis confirmed that no crystalline phases were formed in any of the compositions shown in Table II, indicating that all formed amorphous glasses.

(2) Density and Molar Volume

The effects of substituting oxygen on the density of the glasses are shown in Fig. 2. A significant increase in density is observed as oxygen is replaced by nitrogen, from 2.465 g/cm³ at 0 at.% N to 2.502 g/cm³ at 2.6 at.% N (1.6% increase). As density increases, then there is a decrease in glass molar volume, with a corresponding increase in glass compactness (atomic packing density).

These results confirm previous findings¹⁸ that addition of nitrogen increases cross-linking within the network of oxynitride glasses because oxygen is coordinated to only two tetrahedral silicate units whereas nitrogen is mainly tri-coordinated. For each percentage of oxygen replacement by nitrogen, an equal number of additional cross-links should be introduced into the glass network and, thus, properties that are dependent on increased cross-linking of the glass network should show a linear dependence with nitrogen. This is discussed in the following sections.

(3) Glass-Transition Temperature T_g

Figure 3 shows glass-transition temperature, determined from DTA experiments, as a function of nitrogen content and, as can be seen, there is a fairly linear increase in glass-transition temperature, T_g , as nitrogen content increases. As oxygen is replaced by nitrogen, T_g increases from 618°C at 0 at.% N to 635°C at 2.6 at.% N. A best-fit line through the data gives an empirical expression for T_g versus N:

$$T_g(^{\circ}C) = 618 + 6.37[N] \quad (8)$$

where [N] is N content in at.%. The increase in T_g with N is consistent with previous studies of oxynitride glasses¹⁹⁻²¹ which have shown that N creates extra cross-linkages and stiffens the glass network.

(4) Mechanical Properties

(A) Vickers Microhardness and Young's Modulus:

The Vickers microhardness (Hv) (Load = 4.905 N) as a

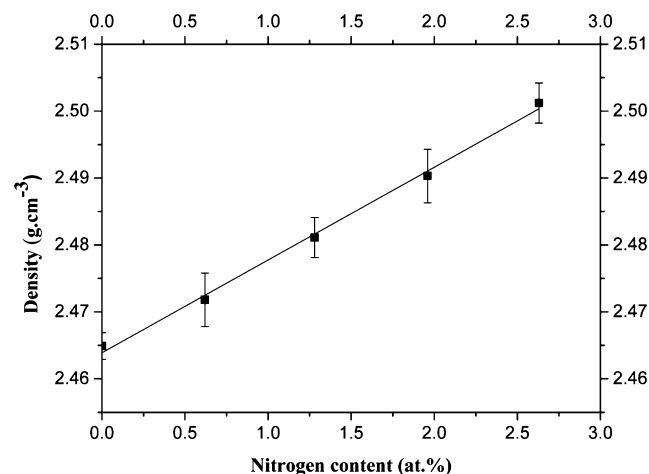


Fig. 2. Density of Na-Ca-Sr-Zn-Sr-Si-O-N_x glasses as a function of nitrogen content.

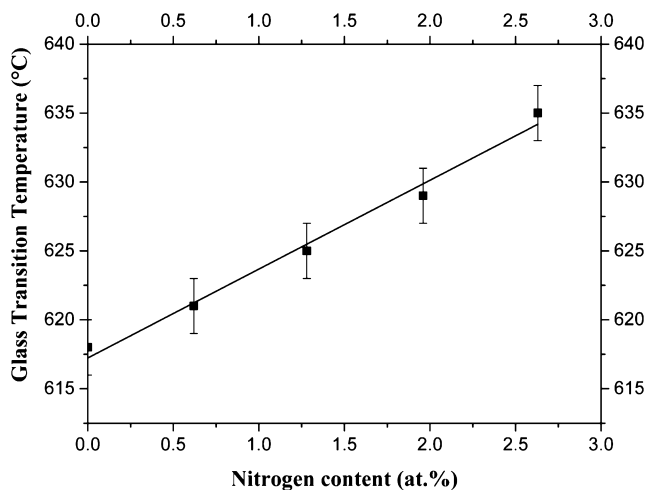


Fig. 3. Glass-transition temperature (T_g) determined by DTA of Na-Ca-Sr-Zn-Si-O-N_x glasses as a function of N content.

function of N content for the glasses is shown in Fig. 4. Hv increases fairly linearly with nitrogen content as reported previously for oxynitride glasses.^{18–21} Microhardness increases with nitrogen content from 4.9 ± 0.3 GPa for 0 at.% N to 5.8 ± 0.4 GPa (15% increase) at 2.6 at.% N. Microhardness can be modeled by the following empirical relationship:

$$H_v(\text{GPa}) = 4.85 + 0.36[\text{N}] \quad (9)$$

where [N] is N content in at.%.

Figure 5 shows Young's modulus (E) as a function of N content for the glasses and, as can be seen, E increases fairly linearly with nitrogen content from 53 ± 3 GPa for 0 at.% N to 83 ± 4 GPa (58% increase) for 2.6 at.% N. Increases in E with N are consistent with results of other studies of oxynitride glasses.^{18,21} The variation in E with N can be modeled by the following empirical relationship:

$$E(\text{GPa}) = 54 + 11[\text{N}] \quad (10)$$

where [N] is N content in at.%.

When comparing these results with those reported earlier for oxynitride and oxyfluoronitride glasses,²⁷ it can be seen from the empirical relationships that the slopes of Hv versus N for these new N-substituted Na-Ca-Sr-Zn-Si glasses and for the previous oxyfluoronitride glasses are identical (~ 0.30 GPa/at.%N). For oxynitride glasses (without fluorine), the slope is somewhat lower but this was thought to be due to the presence of bubbles in the glass. The benefit of nitrogen seems to be similar for the glasses studied here and the previous bioactive glasses containing nitrogen.²⁷

For the Young's modulus, the slope of E versus N (~ 10 GPa/at.%N) is much greater than the slopes of E versus N previously reported for oxynitride and oxyfluoronitride glasses (6.55 and 4.30 GPa/at.%N, respectively). It seems that the influence of nitrogen on mechanical properties is more significant in the current series of glasses and this may be related to the glass structure which is discussed below.

(B) *Vickers Indentation Fracture (VIF) Resistance:* For VIF Resistance calculations, 10 Vickers indentations at eight loads ranging from 1.472 to 4.905 N were carried out on the five glasses. Dimensions of indent diagonals and crack lengths were measured on optical micrographs using the image analysis software ImageJ©. Any tests where cracks did not develop or where chipping occurred were not included in the final analysis.

The first step to calculate VIF resistance was the calculation of the Meyer's index n from the slope of the linear

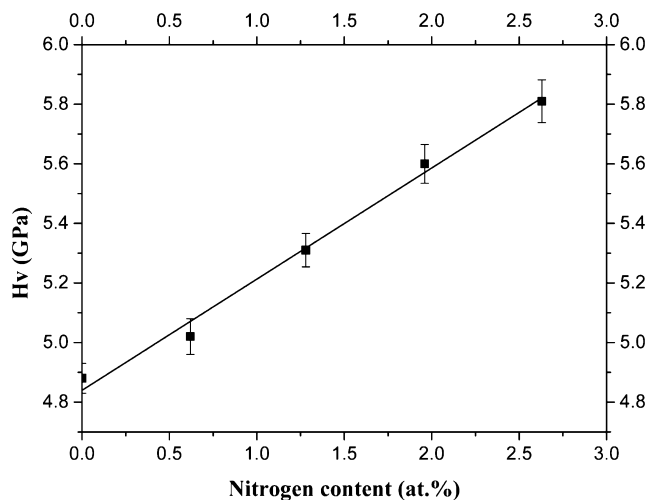


Fig. 4. Vickers microhardness (Load=4.905 N) of Na-Ca-Sr-Zn-Si-O-N_x glasses as a function of nitrogen content.

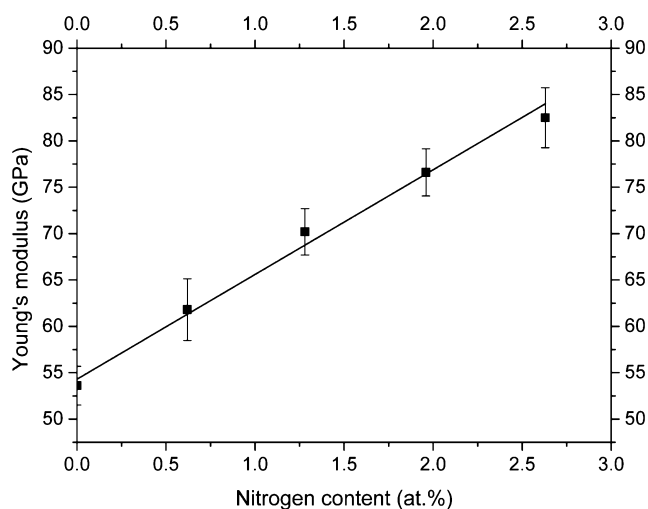


Fig. 5. Young's modulus of Na-Ca-Sr-Zn-Si-O-N_x glasses as a function of nitrogen content.

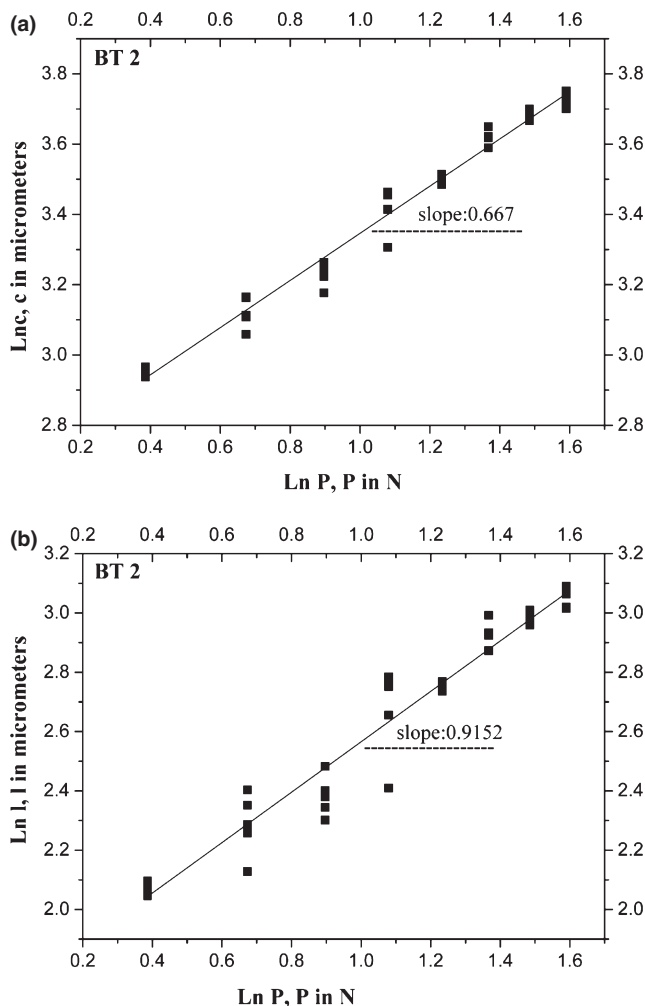
variation $\ln(P) - \ln(a_d)$. To identify the cracking mode the experimental slopes of the $\ln(c) - \ln(P)$ and $\ln(l) - \ln(P)$ linear plots were determined and compared to 0.667 and $2/(1-1/n)$, respectively. The values of Meyer's index and the various slopes of the plots are shown in Table III. As an example, for the BT2 glass, the Meyer's index calculated from the slope of the linear variation $\ln(P) - \ln(a_d)$ is equal to 1.95 and $2/(1-1/n)$ is equal to 0.97. In this particular case, the experimental slopes of (a) $\ln(c) - \ln(P)$ and (b) $\ln(l) - \ln(P)$ linear plots are equal to 0.667 and 0.91, respectively, as shown in Fig. 6. Comparing these values to 0.667 and 1.029, we can conclude that the cracking mode is Radial Median type. For all glasses, as deduced from the results given in Table III, the cracking mode is Radial Median type.

Figure 7 shows the variation in the Vickers indentation fracture resistance, K_{ifr} , with nitrogen content for the glasses. The substitution of nitrogen for oxygen results in an increase in K_{ifr} from 0.91 ± 0.01 MPa·m^{1/2} at 0 at.% N to 1.05 ± 0.01 MPa·m^{1/2} (15% increase) at 2.6 at.% N. The increase in K_{ifr} is not linear and increases much more as nitrogen substitution increases.

Summarizing, the overall increases in mechanical properties with increasing nitrogen content can be related to (i) the increasing average anion coordination with Si when N replaces O^{18–20} and (2) the greater resistance to bending of

Table III. Experimental Data for Na-Ca-Sr-Zn-Si-O-N_x Glasses

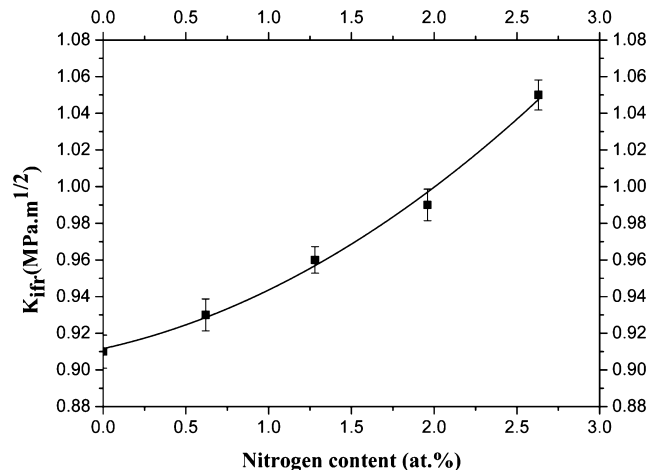
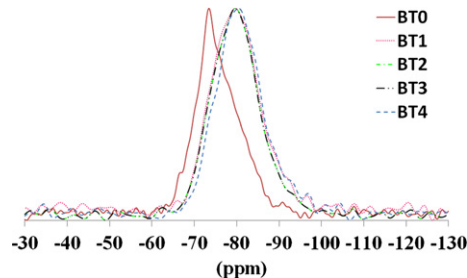
| Glass | BT0 | BT1 | BT2 | BT3 | BT4 |
|-------------------|----------------------|-------|-------|-------|-------|
| At.% N (exp) | 0 | 0.62 | 1.28 | 1.96 | 2.63 |
| Meyer's index n | 1.91 | 1.93 | 1.95 | 2.02 | 1.99 |
| 2(1-1/n) | 0.95 | 0.96 | 0.97 | 1.00 | 0.99 |
| Ln(c)-Ln(P) slope | 0.675 | 0.670 | 0.671 | 0.680 | 0.676 |
| Ln(l)-Ln(P) slope | 0.86 | 0.88 | 0.91 | 0.98 | 0.93 |
| Cracking mode | Radial-medial cracks | | | | |

**Fig. 6.** Calculation of (a) slope of Ln(c)-Ln(P) plot, and (b) slope of Ln(l)-Ln(P) plot for BT2 glass.

the Si-N-Si bond, which results from the more covalent nature of the Si-N bond as compared with the Si-O bond.²¹

(5) ²⁹Si Magic Angle Spinning Nuclear Magnetic Resonance (MAS-NMR) Spectroscopy

Figure 8 shows the ²⁹Si MAS-NMR spectra of glasses doped with different amounts of nitrogen. The variations in chemical shift are indicators of changes in structural parameters such as bond angles and bond lengths in the 1st and 2nd coordination sphere, and of the electronic environment of the probed nuclei. The chemical shift of the main resonance decreases significantly from -75.5 ppm (BT0) for the oxide glass to -80.0 ppm (BT1) as nitrogen is incorporated into the glass and then, with further addition of N, the variation

**Fig. 7.** Vickers indentation fracture resistance (V_{ifr}) of Na-Ca-Sr-Zn-Si-O-N_x glasses as a function of nitrogen content (Ten loads ranging from 1.472 to 4.905 N).**Fig. 8.** ²⁹Si MAS-NMR spectra of Na-Ca-Sr-Zn-Si-O-N_x glasses with different nitrogen contents.

in chemical shift is insignificant with $\delta = -81.0$ ppm for BT4 containing 2.6 at.% N. Therefore, addition of nitrogen to the base oxide glass considerably modifies the medium-range order of silicon indicating a change in the connectivity of the silicate network.

Figure 9 shows the individual ²⁹Si NMR spectra for the five glasses with different nitrogen contents. It can be noted that all spectra are asymmetrical indicating the existence of at least two different structural features involving silicate tetrahedra, Q_{Si}^n , depending on glass composition. The spectra were deconvoluted by using overlapping Gaussian line shapes for the centre bands and the side bands to identify and to quantify the amounts of different Q_{Si}^n species. It was verified, for each glass, that the value of chemical shift for each Q_{Si}^n unit was consistent with the literature^{22,30-35} and their approximate values of FWHM were maintained. In addition, the centers of adjacent Gaussian curves attributed to Q_{Si}^n and Q_{Si}^{n+1} species were separated by at least 7 ppm. The chemical shifts and the relative proportions of Q_{Si}^n entities of the glasses are listed in Table IV.

The BT0 glass without nitrogen consists of 47% Q^1 units and 37% Q^2 units with a minor amount (11%) of Q^0 units. Only for this base oxide glass, the presence of a narrow resonance peak appears on the spectra at -73.2 ppm, attributed to a small amount of nanocrystalline phase although this was not observed by XRD. When nitrogen is introduced into the base glass (BT0), this small peak is no longer seen, indicating a more stable glass, and modifications in the relative proportions of Q^n species are observed with no Q^0 present, increases in Q^2 at the expense of Q^1 units and the appearance of Q^3 units. Initially, with addition of 0.6 at.% N (BT1), the proportion of Q^1 units decreases from 47% to 22%, whereas the proportion of Q^2 units increases from

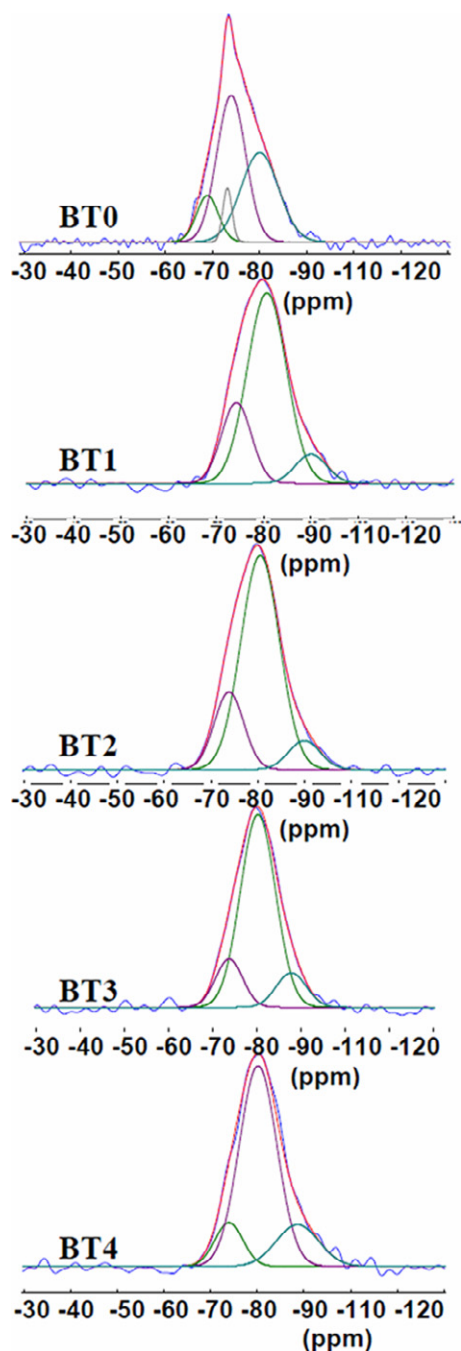


Fig. 9. Deconvolution of ^{29}Si MAS-NMR spectra of Na–Ca–Sr–Zn–Si–O–N_x glasses.

37% to 69% with additionally ~9% Q³ units. The presence of N stabilizes the glass so that no nanocrystalline phase remains as observed previously for oxynitride glasses.^{18,21} Overall, with increase in N from 0% to 2.6 at.% (BT4), the Q¹ species decrease from 47% to 12%, whereas the proportion of Q² units increases from 37% to 71% with additionally 17% Q³. So the addition of nitrogen leads to a greater cross-linking of the silicate network as observed previously for these types of glasses.^{18–21}

(6) Discussion on Network Connectivity

The fraction of nonbridging oxygens (NBOs) can be estimated from the original glass composition and gives a quantitative measure of network connectivity, NC, which is defined as number of bridging oxygens (BO) per tetrahedron (T) or BO/T = 4 – NBO/T.²¹ For a silicate glass, each

NBO must be associated with either a Na⁺ ion or two NBOs must be associated with each M²⁺ cation, where M = Ca, Sr, or Zn.

Zinc oxide in a glass may act as an intermediate ion in the same way as alumina, either as a network forming oxide (Zn^{IV})¹⁰ or as a network modifying oxide in fivefold or sixfold coordination (Zn^{V/VI}).^{12–14} Some reports on bioactive glasses containing zinc oxide (Na₂O–CaO–ZnO–CeO₂–SiO₂ glasses¹¹ or SrO–CaO–ZnO–SiO₂ Ionomer Glasses¹²) suggest that Zn is predominantly in a modifying role, that is, in octahedral coordination, whereas investigations of other glasses (Na₂O–K₂O–CaO–ZnO–SiO₂¹⁰ and Na₂O–RO–Al₂O₃–SiO₂ where R = Zn, Sr, Ba¹³ suggest that Zn behaves more like a network former but with mixed coordination. The ratio of Zn ions in tetrahedral or octahedral coordination depends on the overall glass composition and the amounts of sodium or alkali ions which compensate the charge deficit on the ZnO₄ tetrahedra.¹⁴ A molecular dynamics study of zinc silicate and Na₂O–ZnO–SiO₂ (NZS) glasses³⁶ found that coordination numbers for zinc compare favorably with EXAFS data for both sets of glasses. In the zinc silicate glass, tetrahedral coordination was found but it appeared that zinc acted to disrupt the amorphous silica structure, causing edge-shared oxygens, three-coordinated oxygen, and over-coordinated silicon. In alkali-rich areas of the NZS glasses, zinc was shown to be charge compensated from nearby sodium atoms and formed tetrahedral units to a greater degree. In both sets of glasses, a decrease in the concentration of tetrahedral zinc and an increase in the concentration of both fivefold and sixfold coordinated zinc ions were seen with increasing ZnO content. In more complex bioactive SrO–CaO–MgO–ZnO–SiO₂ glasses containing both CaF₂ and P₂O₅, a molecular dynamics study found that both Zn and Mg were in fivefold coordination.³⁷

Therefore, if Zn acts as an intermediate ion, then network connectivity is given by the following equation:

$$\text{NC} = 4 - \frac{v_{\text{Na}}(N_{\text{Na}}) + v_{\text{M}}(N_{\text{M}}) + v_{\text{Zn}}^{\text{V/VI}}(N_{\text{Zn}}^{\text{V/VI}}) - (N_{\text{Zn}}^{\text{IV}})}{(N_{\text{Zn}}^{\text{IV}} + N_{\text{Si}})} \quad (11)$$

where (N_M) is the no. of ions of type M (= Ca, Sr) and (N_{Zn}^{V/VI}) is the no. of Zn ions in five or sixfold coordination with oxygen (v_M is their valency) and (N_{Zn}^{IV}) is the no. of Zn ions in fourfold coordination. For the oxide glass, if it is assumed that all Zn ions are in tetrahedral coordination, then NC = 3 and if all Zn ions are network modifiers, then NC = 1.

From the NMR data, ignoring the small amount of crystalline phase, this glass consists of approximately 49% Q¹, 39% Q², and 12% Q⁰ units. Therefore, network connectivity:

$$\text{NC} = \sum fQ_{\text{NMR}}^n \times n \quad (12)$$

where fQⁿ_{NMR} is the fraction of Qⁿ units determined from NMR analysis with n = BO/T for this particular species. Therefore, this glass has a network connectivity of:

$$\text{NC} = (0.49 \times 1) + (0.39 \times 2) + (0.12 \times 0) = 1.27 \quad (13)$$

Clearly, from this analysis, Zn atoms exist in different environments, either fourfold, fivefold, or sixfold coordinated to oxygen.^{11,14,15} If it is assumed that only fourfold coordinated Zn ions contribute to the number of BOs then from Eqs. (11) and (13) and NMR analysis, where NC = 1.27, the number of tetrahedral Zn ions, N_{Zn}^{IV}, is given by the following equation:

Table IV. ²⁹Si Isotropic Chemical Shift (δ_{iso}), Full-Width Half Maximum (FWMH), and Relative Abundance (%) of Qⁿ Entities of Na–Ca–Sr–Zn–Si–O–N_x Glasses

| Q _{Siⁿ} entities | | Q ⁰ | Q ^{1†} | Q ¹ | Q ² | Q ³ |
|--------------------------------------|--------------------------------------|----------------|-----------------|----------------|----------------|----------------|
| BT0 | δ_{iso} (ppm ± 1) | −68.9 | −73.2 | −74.0 | −80.0 | |
| | FWMH (ppm ± 0.5) | 5.4 | 2.3 | 7.2 | 9.4 | |
| | % Q ⁿ (± 5) | 11 | 5 | 47 | 37 | |
| BT1 | δ_{iso} (ppm ± 1) | | | −74.3 | −80.7 | −89.9 |
| | FWMH (ppm ± 0.5) | | | 7.4 | 9.7 | 7.9 |
| | % Q ⁿ (± 5) | | | 22 | 69 | 9 |
| BT2 | δ_{iso} (ppm ± 1) | | | −73.8 | −80.5 | −89.9 |
| | FWMH (ppm ± 0.5) | | | 7.4 | 9.7 | 7.9 |
| | % Q ⁿ (± 5) | | | 20 | 72 | 8 |
| BT3 | δ_{iso} (ppm ± 1) | | | −73.7 | −80.2 | −87.8 |
| | FWMH (ppm ± 0.5) | | | 7.3 | 9.4 | 8 |
| | % Q ⁿ (± 5) | | | 14 | 74 | 12 |
| BT4 | δ_{iso} (ppm ± 1) | | | −73.9 | −80.2 | −88.6 |
| | FWMH (ppm ± 0.5) | | | 7.1 | 9.5 | 10.7 |
| | % Q ⁿ (± 5) | | | 12 | 71 | 17 |

[†]Attributed to the crystalline phase.

$$1.27 = 4 - [(2 \times 10) + 2(10 + 20 + (20 - N_{\text{Zn}}^{\text{IV}})) - N_{\text{Zn}}^{\text{IV}}] / (40 + N_{\text{Zn}}^{\text{IV}}) \quad (14)$$

Thus, $N_{\text{Zn}}^{\text{IV}} = 1.88$ which suggests that 1.88/20 = ~9.4% of the Zn ions are in tetrahedral coordination and act as glass formers, whereas ~90% of the Zn ions are in fivefold or sixfold coordination with oxygen and do not provide BOs.

When N replaces O in these glasses, increased cross-linking within the glass structure occurs as two-coordinated BO atoms are replaced by three-coordinated nitrogen atoms, each N providing one extra bridging option compared with oxygen. N may also provide two-coordinated partially bridging N atoms, as in: $\equiv\text{Si}-\text{N}^--\text{Si}\equiv$

When N is present, then each N (N_{N}) provides an extra bridging option to oxygen so that:

$$\text{NC} = 4 - [(v_{\text{Na}}(N_{\text{Na}}) + v_{\text{M}}(N_{\text{M}}) - (N_{\text{Zn}}^{\text{IV}}) - (N_{\text{N}})] / (N_{\text{Si}} + N_{\text{Zn}}^{\text{IV}}) \quad (15)$$

For different N contents:

$$\text{NC} = 4 - [(2 \times 10) + 2[10 + 20 + (20 - N_{\text{Zn}}^{\text{IV}})] - N_{\text{Zn}}^{\text{IV}} - (N_{\text{N}})] / (40 + N_{\text{Zn}}^{\text{IV}}) \quad (16)$$

From NMR data, the glasses containing N all have similar spectra with increasing proportions of Q² units with addition of N. For the glass containing 2.6 at.% N (BT4), the Q¹ species decrease from 47% to 12% while the proportion of Q² units increases from 37% to 72% with the appearance of ~17% Q³. Therefore, from Eq. (12), this glass should have a network connectivity of:

$$\text{NC} = (0.12 \times 1) + (0.72 \times 2) + (0.17 \times 3) = 2.07 \quad (17)$$

and from Eq. (16), $N_{\text{Zn}}^{\text{IV}} = 8.15$ and therefore 8.15/20 = ~40% of Zn ions may be in tetrahedral coordination. Calculation of network connectivity for the other N-containing glasses gives values as follows: BT1: NC = 1.86; BT2: NC = 1.88; BT3: NC = 1.97. With network connectivity of close to two, then the overall structure would be equivalent to $[\text{SiO}_3]^{2-}$ chains.

The significant change in the NMR spectra when even a small amount of N is substituted for oxygen would suggest

that the glasses containing N have quite different structural features than the oxide glass and that the role of Zn as a glass former becomes more significant when N is present. It should be noted that the $[\text{SiO}_3\text{N}]^{5-}$ group requires the presence of a cation locally to balance an extra negative charge compared with SiO_4 tetrahedra and therefore the situation is very similar to that for an $[\text{AlO}_4]^{5-}$ tetrahedron within the network. Therefore, oxynitride glasses containing SiO_3N groups can accommodate more “modifiers” in “network dwelling” sites than the equivalent oxide glasses. Thus, Zn ions may have a preferential role and thus the proportion of Zn ions in sites where no NBOs are created increases with N content and network connectivity increases as modifying ions provide charge compensation for the tetrahedra. A similar situation was found previously for Mg in oxynitride glasses which also takes on tetrahedral coordination when N is present^{18,21} Overall, the predominant Qⁿ structures for the N-containing glasses were confirmed by MAS-NMR as mainly Q² with Q¹ and also some Q³ units and from the network connectivity calculations, it is clear that up to ~40% of Zn ions are preferentially in fourfold coordination because of the presence of 2.6 at.% nitrogen.

(7) Potential as Glass Component of Glass-Polyalkenoate Cement in Orthopedics

Hardness and Young's modulus were found to increase linearly with nitrogen content. The modest increase (~15%) in indentation fracture resistance with 2.6 at.% N also suggests a strengthening of the glass when N is substituted for O. These observations, combined with structural analysis by NMR, indicate that the incorporation of nitrogen, which is tri-coordinated with silicon compared with twofold coordination for oxygen, results in extra cross-linking and stiffening of the glass network. If these glasses were to be used in biomedical applications, then N would help to strengthen the glass and the presence of Zn in tetrahedral coordination would increase the chemical durability at normal body pH (~7).¹⁰ As these glass compositions are close to those being considered for the glass component of a GP cement^{9,12} which is reacted with PAA, then the Zn in these glasses aids in their dissolution at low pH so while the higher network connectivity might mitigate against reaction of the glass, the NC is still low enough that reaction should occur. The resulting cement containing N should be stronger and would increase the load bearing ability in the skeleton while the Zn would facilitate glass degradation over time and offer antibacterial properties.³⁸

The use of zinc-containing cements might also permit incorporation of antibiotics at considerably lower concentrations

than are currently necessary to avoid bacterial infections in Total Hip Arthroplasty (THA).^{39,40} Bacterial infection after THA is a serious complication of hip replacement surgery that frequently necessitates revision surgeries. This would not only reduce weakening of the cement but, due to presence of both antibacterial zinc and the antibiotics, might be expected to reduce the rate at which antibiotic resistant bacteria arise.^{39,40} The use of zinc-containing oxynitride glasses as the glass component of the cement appears to have potential and may be particularly effective if used in conjunction with impregnated antibiotics.

IV. Conclusions

Glasses with molar composition: $10\text{Na}_2\text{O}-10\text{CaO}-20\text{SrO}-20\text{ZnO}-(40-3x)\text{SiO}_2-x\text{Si}_3\text{N}_4$ ($x = 1, 2, 3, 4$ is the no. of moles of Si_3N_4) have been synthesized and characterized. The following conclusions can be made regarding the effect of composition on properties and structure:

1. Density increases with nitrogen substitution for oxygen which is a result of the higher compactness of the glass network and therefore a lower molar volume.
2. Glass-transition temperature, hardness, and Young's modulus all increase linearly with nitrogen content which indicates that the incorporation of nitrogen, which is tri-coordinated with silicon compared with twofold coordination for oxygen, results in extra cross-linking and stiffens the glass network. A modest increase (~15%) in indentation fracture resistance with substitution of 2.6 at.% N occurs according to a power law relationship.
3. The characterization of these N-substituted Na-Ca-Sr-Zn-Si bioactive glasses using ²⁹Si MAS-NMR has shown that the increase in connectivity of the glass network can be explained by the formation of an increasing number of Q² units with increasing nitrogen content, thus forming extra bridging anions at the expense of Q¹ units. A small proportion (~9%) of Zn ions are found to be in tetrahedral coordination in the base oxide glass and the proportion of these increases to ~40% with substitution of nitrogen for oxygen.
4. While higher network connectivity may decrease glass degradation, the presence of Zn should ensure that reaction of the glass with PAA occurs at low pH to form stronger GP cements which may have potential in orthopedic load-bearing applications.

Acknowledgments

The authors gratefully acknowledge the useful contributions of Séverine Belayer (Ecole Nationale Supérieure de Chimie de Lille, ENSCL, France).

References

- ¹L. L. Hench, "Bioceramics—from Concept to Clinic," *J. Am. Ceram. Soc.*, **74**, 1487–510 (1991).
- ²L. L. Hench, R. J. Splinter, W.-C. Allen, and T. K. Greenlee, "Mechanisms of Interfacial Bonding Between Ceramics and Bone," *J. Biomed. Mater. Res. Symp.*, **2**, 117–41 (1971).
- ³L. L. Hench and J. K. West, "Biological Applications of Bioactive Glasses," *Life Chem. Rep.*, **13**, 187–241 (1996).
- ⁴S. Fujibayashi, M. Neo, H. Kim, T. Kokubo, and T. Nakamura, "A Comparative Study Between *In Vivo* Bone In-Growth and *In Vitro* Apatite Formation on $\text{Na}_2\text{O}-\text{CaO}-\text{SiO}_2$ Glasses," *Biomaterials*, **24**, 1349–56 (2003).
- ⁵R. Hill, "An Alternative View of the Degradation of Bioglass," *J. Mater. Sci. Letts*, **15**, 1122–5 (1996).
- ⁶L. M. Jonck, C. J. Grobelaar, and H. Strating, "The Biocompatibility of Glass-Ionomer Cement in Joint Replacement: Bulk Testing," *Clin. Mater.*, **4**, 85–107 (1989).
- ⁷G. Geyer and J. Helms, "Ionomer-Based Bone Substitute Entomologic Surgery," *Eur. Arch. Oto-Rhino Laryngol.*, **250**, 253–6 (1993).
- ⁸S. G. Griffin and R. Hill, "Influence of Glass Composition on the Properties of Glass Polyalkenoate Cements. Part I: Influence of Aluminium to Silicon Ratio," *Biomaterials*, **17**, 1579–86 (1999).

⁹D. Boyd and M. R. Towler, "The Processing, Mechanical Properties and Bioactivity of Zinc Based Glass Ionomer Cements," *J. Mater. Sci. Mater. Med.*, **9**, 843–50 (2005).

¹⁰X. Chen, D. S. Brauer, N. Karpukhina, R. D. Waite, M. Barry, I. J. McKay, and R. G. Hill, "Smart" Acid-Degradable Zinc-Releasing Silicate Glasses," *Mater. Letts*, **126** [1] 278–80 (2014).

¹¹X. F. Zhang, S. Kehoe, S. K. Adhi, T. G. Ajithkumar, S. Moane, H. O'Shea, and D. Boyd, "Composition–Structure–Property (Zn^{2+} and Ca^{2+} ion Release) Evaluation of Si–Na–Ca–Zn–Ce Glasses: Potential Components for Nerve Guidance Conduits," *Mater. Sci. Eng., C*, **31** [3] 669–76 (2011).

¹²D. Boyd, M. R. Towler, S. Watts, R. G. Hill, A. W. Wren, and O. M. Clarkin, "The Role of Sr^{2+} on the Structure and Reactivity of $\text{SrO}-\text{CaO}-\text{ZnO}-\text{SiO}_2$ Ionomer Glasses," *J. Mater. Sci. Mater. Med.*, **2**, 953–7 (2008).

¹³M. M. Smedskjaer, R. E. Youngman, and J. C. Mauro, "Impact of ZnO on the Structure and Properties of Sodium Aluminosilicate Glasses: Comparison with Alkaline Earth Oxides," *J. Non-Cryst. Solids*, **381** [1] 58–64 (2013).

¹⁴G. Calas, L. Cormier, L. Galoisy, and P. Jollivet, "Structure–Property Relationships in Multicomponent Oxide Glasses," *Comp. Rendu Chimie*, **5**, 831–43 (2002).

¹⁵G. Lusvardi, G. Malavasi, L. Menabue, M. C. Menziani, U. Segre, M. M. Carnasciali, and A. Ubalini, "A Combined Experimental and Computational Approach to $(\text{Na}_2\text{O})_{1-x}\text{CaO}(\text{ZnO})_x2\text{SiO}_2$ Glasses Characterization," *J. Non-Cryst. Solids*, **345–346** [15] 710–4 (2004).

¹⁶K. Fujikura, N. Karpukhina, T. Kasuga, D. S. Brauer, R. G. Hill, and R. V. Law, "Influence of Strontium Substitution on Structure and Crystallisation of Bioglass® 45S5," *J. Mater. Chem.*, **15**, 7395–402 (2012).

¹⁷A. W. Wren, A. Coughlan, F. R. Laffir, and M. R. Towler, "Comparison of a $\text{SiO}_2-\text{CaO}-\text{ZnO}-\text{SrO}$ Glass Polyalkenoate Cement to Commercial Dental Materials: Glass Structure and Physical Properties," *J. Mater. Sci. Mater. Med.*, **7**, 271–80 (2013).

¹⁸S. Hampshire, R. A. L. Drew, and K. H. Jack, "Oxynitride Glasses," *Phys. Chem. Glasses*, **26**, 182–6 (1985).

¹⁹S. Hampshire, "Oxynitride Glasses," *J. Eur. Ceram. Soc.*, **28**, 1475–83 (2008).

²⁰S. Hampshire and M. J. Pomeroy, "Oxynitride Glasses," *Int. J. Appl. Ceram. Technol.*, **5**, 155–63 (2008).

²¹P. Becher, S. Hampshire, M. J. Pomeroy, M. Hoffmann, M. Lance, and R. Satet, "An Overview of the Structure and Properties of Silicon-Based Oxynitride Glasses," *Int. J. Appl. Glass Sci.*, **2**, 63–83 (2011).

²²A. Bachar, C. Mercier, A. Tricoteaux, A. Leriche, C. Follet, M. Saadi, and S. Hampshire, "Effects of Addition of Nitrogen on Bioglass Properties and Structure," *J. Non-Cryst. Solids*, **358**, 693–701 (2012).

²³A. R. Hanifi, C. M. Crowley, M. J. Pomeroy, and S. Hampshire, "Bioactivity Potential of Calcium Aluminosilicate Glasses and Glass-Ceramics Containing Nitrogen and Fluorine," *J. Mater. Sci.*, **49** [13] 4590–4 (2014).

²⁴M. J. Pomeroy, E. Nestor, R. Ramesh, and S. Hampshire, "Properties and Crystallisation of Rare Earth SiAlON Glasses Containing Mixed Trivalent Modifiers," *J. Am. Ceram. Soc.*, **88**, 875–81 (2005).

²⁵M. Roskosh, M. A. Bouhifd, A. P. Jephcoat, B. Marty, and B. O. Mysen, "Nitrogen Solubility in Molten Metal and Silicate at High Pressure and Temperature," *Geoch. Cosmo. Acta*, **121**, 15–28 (2013).

²⁶D. B. Marshall, T. Noma, and A. G. A. Evans, "Simple Method for Determining Elastic Modulus to Hardness Ratios Using Knoop Indentation Measurements," *J. Am. Ceram. Soc.*, **65**, C175–6 (1980).

²⁷A. Bachar, C. Mercier, A. Tricoteaux, S. Hampshire, A. Leriche, and C. Follet, "Effect of Nitrogen and Fluorine on Mechanical Properties and Bioactivity in Two Series of Bioactive Glasses," *J. Mech. Behav. Biomed. Mater.*, **23**, 133–48 (2013).

²⁸D. Chicot and A. Tricoteaux, "Mechanical Properties of Ceramics by Indentation: Principle and Applications"; pp.115–54 in *Ceramic Materials*, Edited by W. Wunderlich, InTech-Sciyo, Rijeka, Croatia, 2010.

²⁹D. Massiot, F. Fayon, M. Capron, I. King, S. Le Calvé, B. Alonso, J. O. Durand, B. Bujoli, Z. Gan, and G. Hoatson, "Modelling One and Two-Dimensional Solid-State NMR Spectra," *Magn. Reson. Chem.*, **40**, 70–6 (2002).

³⁰K. J. D. Mackenzie and M. E. Smith, *Multinuclear Solid-State NMR of Inorganic Materials*. Pergamon-Elsevier Science, Oxford, UK, 2002.

³¹E. Schneider, J. F. Stebbins, and A. Pines, "Speciation and Local Structure in Alkali and Alkaline Earth Silicate Glasses: Constraints from ²⁹Si NMR Spectroscopy," *J. Non-Cryst. Solids*, **89** [3] 371–83 (1987).

³²G. Engelhardt, "Multinuclear Solid-State NMR in Silicate and Zeolite Chemistry," *Tr. An. Chem.*, **8** [9] 343–7 (1989).

³³H. Maekawa, T. Maekawa, K. Kawamura, and T. Yokokawa, "The Structural Groups of Alkali Silicate Glasses Determined from ²⁹Si MAS-NMR," *J. Non-Cryst. Solids*, **127** [1] 53–64 (1991).

³⁴M. W. G. Lockyer, D. Holland, and R. Dupree, "NMR Investigation of the Structure of Some Bioactive and Related Glasses," *J. Non-Cryst. Solids*, **188** [31] 207–19 (1995).

³⁵J. Schneider, V. R. Mastelaro, E. D. Zanotto, B. A. Shakhmatkin, N. M. Vedishcheva, A. C. Wright, and H. Panepucci, "Qⁿ Distribution in Stoichiometric Silicate Glasses: Thermodynamic Calculations and ²⁹Si High Resolution NMR Measurements," *J. Non-Cryst. Solids*, **325** [1–3] 164–78 (2003).

³⁶A. B. Rosenthal and S. H. Garofalini, "Structural Role of Zinc Oxide in Silica and Soda-Silica Glasses," *J. Am. Ceram. Soc.*, **70** [11] 821–6 (1987).

³⁷S. Kapoor, A. Goel, A. Tilocca, V. Dhuna, G. Bhatia, K. Dhuna, and J. M. F. Ferreira, "Role of Glass Structure in Defining the Chemical Dissolution

Behavior, Bioactivity and Antioxidant Properties of Zinc and Strontium Co-Doped Alkali-Free Phosphosilicate Glasses,” *Acta Biomater.*, **10** [7] 3264–78 (2014).

³⁸D. Cummins, “Zinc Citrate/Triclosan: A New Anti-Plaque System for the Control of Plaque and the Prevention of Gingivitis: Short-Term Clinical and Mode of Action Studies,” *J. Clin. Periodontol.*, **18**, 455–61 (1991).

³⁹T. N. Joseph, A. L. Chen, and P. E. Di Cesare, “Use of Antibiotic-Impregnated Cement in Total Joint Arthroplasty,” *J. Am. Acad. Orthop. Surg.*, **11**, 38–47 (2003).

⁴⁰K. Yamamoto, N. Miyagawa, T. Masaoka, Y. Katori, T. Shishido, and A. Imakiire, “Clinical Effectiveness of Antibiotic-Impregnated Cement Spacers for the Treatment of Infected Implants of the Hip Joint,” *J. Orthop. Sci.*, **8** [6] 823–8 (2003). □